

# Analysis of longitudinal dynamic stability of tandem wing aircraft

Marcin Figat and Agnieszka Kwiek

Aircraft Design Division, Faculty of Power and Aeronautical Engineering, Institute of Aeronautics and Applied Mechanics, Warsaw University of Technology, Warsaw, Poland

## Abstract

**Purpose** – Tandem wing aircrafts belong to an unconventional configurations group, and this type of design is characterised by a strong aerodynamic coupling, which results in lower induced drag. The purpose of this paper is to determine whether a certain trend in the wingspan impact on aircraft dynamic stability can be identified. The secondary goal was to compare the response to control of flaps placed on a front and rear wing.

**Design/methodology/approach** – The aerodynamic data and control derivatives were obtained from the computational fluid dynamics computations performed by the MGAERO software. The equations of aircraft longitudinal motion in a state space form were used. The equations were built based on the aerodynamic coefficients, stability and control derivatives. The analysis of the dynamic stability was done in the MATLAB by solving the eigenvalue problem. The response to control was computed by the step response method using MATLAB.

**Findings** – The results of this study showed that because of a strong aerodynamic coupling, a nonlinear relation between the wing size and aircraft dynamic stability properties was observed. In the case of the flap deflection, stronger oscillation was observed for the front flap.

**Originality/value** – Results of dynamic stability of aircraft in the tandem wing configuration can be found in the literature, but those studies show outcomes of a single configuration, while this paper presents a comprehensive investigation into the impact of wingspan on aircraft dynamic stability. The results reveal that because of a strong aerodynamic coupling, the relation between the span factor and dynamic stability is nonlinear. Also, it has been demonstrated that the configuration of two wings with the same span is not the optimal one from the aerodynamic point of view.

**Keywords** Tandem wing, Optimisation, Dynamic stability, Response to control, Unconventional configuration

**Paper type** Research paper

## Nomenclature

### Symbols

$b_F$	= wingspan of the front wing [m];
$b_F/b_R$	= span factor, ratio of the front wingspan to rear wingspan [–];
$b_R$	= wingspan of the rear wing [m];
$C_D$	= drag coefficient [–];
$C_{Dq}$	= derivative of drag coefficient with respect to pitch rate [1/rad];
$C_L$	= lift coefficient [–];
$C_{Lq}$	= derivative of lift coefficient with respect to pitch rate [1/rad];
$C_{MY}$	= pitching moment coefficient [–];
$C_{Myq}$	= derivative of pitching moment coefficient with respect to pitch rate [1/rad];
$dC_L/d\delta$	= derivative of lift coefficient with respect to flap deflection [1/rad];
$dC_{MY}/d\delta$	= derivative of pitching moment coefficient with respect to flap deflection [1/rad];
$I_Y$	= moment of inertia [kg m <sup>2</sup> ];
$m$	= mass [kg];

MAC	= mean aerodynamic chord [m];
$q$	= pitch rate [1/rad];
$S$	= wing area [m <sup>2</sup> ];
$T_{1/2}$	= time to half damping [s];
$U$	= forward speed [m/s];
$W$	= vertical speed [m/s];
$\alpha$	= angle of attack [degrees];
$\delta$	= angle of flap deflection [degrees];
$\Delta s$	= wings stagger; and
$\theta$	= pitch angle.

### Subscript

F	= front wing; and
R	= rear wing.

### Abbreviations

AoA	= angle of attack;
CFD	= computational fluid dynamics;

The current issue and full text archive of this journal is available on Emerald Insight at: <https://www.emerald.com/insight/1748-8842.htm>



Aircraft Engineering and Aerospace Technology  
95/9 (2023) 1411–1422  
Emerald Publishing Limited [ISSN 1748-8842]  
[DOI 10.1108/AEAT-11-2022-0328]

© Marcin Figat and Agnieszka Kwiek. Published by Emerald Publishing Limited. This article is published under the Creative Commons Attribution (CC BY 4.0) licence. Anyone may reproduce, distribute, translate and create derivative works of this article (for both commercial and non-commercial purposes), subject to full attribution to the original publication and authors. The full terms of this licence may be seen at <http://creativecommons.org/licenses/by/4.0/legalcode>

Received 28 November 2022  
Revised 14 March 2023  
20 April 2023  
Accepted 20 April 2023

CG = centre of gravity;  
 UAV = unmanned aerial vehicle; and  
 VTOL = vertical take-off and landing.

## Introduction

The current trend of the sustainable development of transport puts more emphasis on pollution reduction, which is strongly related to aircraft's drag characteristics. The possibilities of design of more sustainable aircraft in a conventional configuration are limited. Moreover, further enhancement of a conventional configuration from the aerodynamic point of view seems to be exhausted. Therefore, lots of researchers are searching for a more effective configuration by turning to non-conventional configurations (Bravo-Mosquera *et al.*, 2022; Goetzendorf-Grabowski, 2023) like biplane (Goraj *et al.*, 2001), tandem wing (Goetzendorf-Grabowski and Figat, 2017), joined wing (Galinski *et al.*, 2018), flying wing (Mieloszyk *et al.*, 2020), three surfaces configuration (Goetzendorf-Grabowski and Antoniewski, 2016), delta wing (Gudmundsson, 2014), etc.

One of the more interesting, but not very popular, aircraft configurations is a tandem wing configuration. The first planes in this configuration were built at the beginning of the 20th century but the first mention of such a configuration dates back to the 15th century (Bottomley, 1977). Interesting examples of such designs are presented in Figure 1.

Figure 1A shows a design from the last years of the Second World War (Brinkworth, 2016). Figures 1B and 1C show aircrafts flown in the post-war years. But the Pou du Ciel "Flying Flea" aircraft is the developed version of the project that was started in 1933. Figure 2 presents the most interesting examples of contemporary aircrafts like Dragonfly MKII, Rutan Quickie and Proteus. It should be mentioned that all the presented aircraft are prototypes or homemade structures. Recently, the tandem wing configuration became popular in UAV aircrafts, especially with VTOL capabilities (Filho and Belo, 2018).

The tandem wing configuration can be helpful in improving aircrafts performance because of generation of lower induced drag and higher lift (Stinton, 2001; Munk, 1922). This distinguishes it from conventional configurations and may be an interesting alternative to a classical configuration. But the main challenge associated with designing this configuration is a strong aerodynamic coupling problem. Generation of lift, drag and pitching moment highly depends on both wings and its mutual aerodynamic interference. This implies that designing an aircraft in this configuration requires more analysis and computations to get benefits of such a configuration.

**Figure 1** Miles M.39B in flight (on the left, reprinted from Brinkworth, 2016, picture under the Creative Commons Attribution 3.0 license), Curtiss-Wright X-19 experimental VTOL plane (in the middle, public domain picture by USAF) and Mignet HM.380 Pou du Ciel "Flying Flea" (on the right, picture by Joost J. Bakker, picture under CC BY 2.0)



**Figure 2** Dragonfly Mk II (on the left, photo by Robert Frola, under GNU Free Documentation License 1.3), The Rutan Quickie Q2 (on the right, courtesy of Scaled Composites, LLC.) and Proteus (at the bottom, photo by Tom Tschida in public domain, NASA Dryden Flight Research Centre Photo Collection)



## Background

As it was mentioned, aircrafts designed in a tandem wing configuration belong to a huge group of unconventional configurations. This type of design in comparison to others is characterised by a strong aerodynamic coupling, which results in lower induced drag (Chou *et al.*, 2013; Munk, 1922; Stinton, 2001). The classic tandem wing configuration consists of two similar span wings placed on the same level (Figure 1 – in the middle). But this configuration can be improved by changing the vertical and horizontal wings' positions towards each other or changing both wingspans independently. All these modifications were intended to improve the performance of the aircraft. Examples of such configurations are presented in Figures 1 and 2.

Both wings are responsible for lift generation, and both significantly impact the aircraft stability and controllability. Control surfaces may be located on both wings – at the front and/or rear. They can work as elevators and ailerons. The former is used to obtain the trim condition and to ensure the longitudinal control, as well as to increase the lift (as a high lift devices). The latter are used to control the roll motion.

For all the cases of tandem wing configuration, their aerodynamic and flight mechanics analysis is a complex problem. Therefore, the necessary design methodology needs to involve optimisation process (Mieloszyk, 2017). Main geometrical features like span, wing chord, wing stager, gap and decalage should be used as independent variables. Moreover,

the choice of the proper flaps' deflection strategy is very important. In the case of multi-surfaces aircrafts, there is more than one possible set of deflections to ensure the trim condition (Figat, 2022). In the case of the tandem wing, the deflection has a significant impact on the L/D; therefore, the optimal solution depends on the implemented strategy.

However, in the case of aircrafts with a strong aerodynamic coupling, the optimisation process cannot be only limited to aerodynamic features, but multidisciplinary constrains such as dynamic stability must be included as well (Mieloszyk *et al.*, 2017; Goetzendorf-Grabowski, 2017). In the case of a classic configuration, simple analytical or empirical methods can be implemented to reduce the computation cost and enhance the optimisation process, especially during an early stage of the design (Stinton, 2001; Gudmundsson, 2014). The possible solution to reduce the computation time is the use of a low-order software like the one based on a potential flow. But in the case of the aircraft that is characterised by a strong aerodynamic coupling, using low-order software is not always possible because of flow model simplifications. Such an example is the tandem wing, where the wings proximity results in the downwash exerting a significant influence on the aircraft aerodynamic, and there is a mutual interference of both wings, which cannot be neglected.

In the literature, the studies of tandem wing configurations were focused mainly on the aerodynamic analysis of a complex system and their mutual interference. For example, Gao *et al.* (2017) investigated the aerodynamics of two UAV with a different gap and feasibility of folding the configuration. The wind tunnel results measured for the UAV model in the tandem wing configuration with different staggers, dihedrals and wingspans are presented in Masko *et al.* (2014). Also, there were a few two-dimensional studies into the position of aerofoils in the tandem configuration. The results of the numerical computation of aerofoils placed on the same level and at the same distance correspond to a wing stagger equal to 0.5 are presented in Muyao and Hongyi (2021). This study showed that the rear aerofoil generates more lift and less drag, which is associated with the flow behaviour after the first wing. Also, the numerical study of tandem aerofoil with a different stagger, gap and decalage is presented in Jinbin *et al.* (2016). This study reveals that the decalage has the most important effect on aerofoil aerodynamics, while the stagger and gap cause a strong interference only where these are relatively small.

The second important issue which needs to be addressed during a tandem wing configuration design is analysis of aircraft static and dynamic stability. The results of static stability of the tandem wing aircraft with two different wings' configurations were analysed in Kostić *et al.* (2022). The dynamic analysis, if present in the literature, was made for sample configurations only (Goetzendorf-Grabowski *et al.*, 2017). The problem of a vertical position of the bi-plane wings and its impact on the dynamic stability was investigated in Goraj *et al.* (1998). The results of aircraft dynamic modelling for a single aircraft configuration but different flight conditions are shown in Cheng *et al.* (2021).

Typically, the problem of aircraft dynamic stability can be estimated by solving nonlinear equations of motion or by solving the eigenvalues problem of linearised equations of motion (Pobikrowska and Goetzendorf-Grabowski, 2019). The equations can be linearised under the small disturbance

theory and then aerodynamic forces and moments can be described by the Taylor series (Cook, 1997). In the case of unconventional configurations, the problem of estimation of aircraft flight dynamics by solving the eigenvalues problem was considered in Goetzendorf-Grabowski *et al.* (2016), Goraj (2014) and Mieloszyk *et al.* (2020).

## Research aims and objectives

The goal of this paper is to check the impact of the wingspan configuration on the static and dynamic stability of the aircraft in the tandem wing configuration. The research question is to determine whether a visible trend in the wingspan impact on aircraft dynamic stability can be identified. If such a kind of trend existed, then an analytical model could be created or at least the number of possible cases for analysis could be narrowed down. This could be helpful in speeding up the process of design and optimisation of an aircraft in the tandem wing configuration.

The second goal was to compare the aircraft step response, where two scenarios were considered for the front and rear flaps. The step deflections of flaps on each wing were considered separately. The comparison of flap responses is presented for two cases. The first case when only the control surface on the front wing is engaged against the second case when the control surface on the rear wing is engaged.

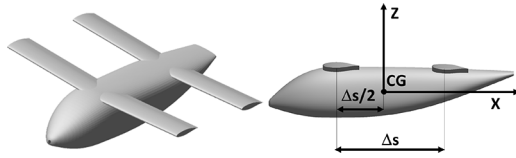
In this paper, a study of ten different aircraft configurations of the tandem wing aircraft is presented. The geometrical parameters varying in each model are the wingspans of the front and rear wing. Firstly, the results of the aerodynamic analysis are shown, including the aerodynamic coefficients like lift, drag and pitching moment of the complete aircraft, in the clean configuration. Moreover, the contribution to aerodynamic coefficients of both wings is presented. Next, the control derivatives of both wings' flaps were computed. The received data were used to establish the trim condition for the analysed aircraft. The last part of the aerodynamic analysis was devoted to calculations of the wing's span impact on the longitudinal stability derivatives like  $C_{Lq}$ . Finally, the outcomes of investigation into the longitudinal dynamic stability and response to control were analysed.

## Research object – Aircraft presentation

In this study, a tandem wing aircraft designed within the PPLANE project (PPlane, 2009; Figat *et al.*, 2010) was used as a research object (Goetzendorf-Grabowski *et al.*, 2017). The original design was equipped with tilted rotors installed at the wings tips, but to analyse the pure aerodynamic impact of wings on aerodynamics and dynamic stability, those rotors were neglected in the numerical model. The presented analysis is restricted to the longitudinal motion only; therefore, the vertical fin installed at the back of the fuselage (Goetzendorf-Grabowski *et al.*, 2017) was neglected as well.

The numerical model that was used in this study is presented in Figure 3. The high wing configuration with the wing with the same aerofoil without any aerodynamic and geometric twist was chosen. The incidence angle of the wing was applied only to the rear wing, and it was assumed to be equal to  $3^\circ$ . The positions of the wings were fixed and corresponded to the wing stagger equal to  $\Delta s = 1.5$  (Figure 3). Moreover, the lengths of the wings' chords were fixed as well. The front wingspan and

**Figure 3** Simplified model of the PPLANE aircraft used in the presented study (on the left). Side view of the aircraft includes definition of the wing stager (on the right)



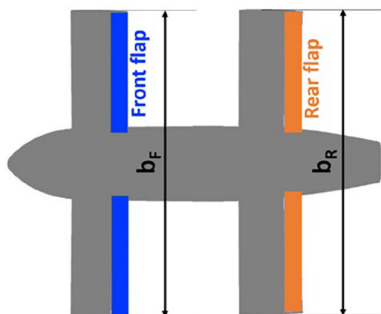
Source: Figure by authors

the rear wingspan were the only parameters that were not constant (Figure 4). The lengths of both wingspans were selected so that the change of the wingspans does not change the reference area. The wingspan change affects the isolated wing's area, but the sum of both wings' area is always the same. It means that for all the cases, the reference area defined as a sum of both wings' area was constant. If the wingspan of the front wing increased, then the wingspan of the rear wing decreased to ensure that the sum of the wings area remains constant. The flaps were placed on both wings (Figure 4) and could act as an elevator.

### Research methodology

This section describes the research methodology, providing a general overview of the approach. Detailed information about the implemented models and software can be found in the later sections. In this paper, all the presented results and analyses are restricted to the longitudinal motion only. To address the research question, the study was divided into four main stages. The first step included aerodynamic computation of all models by the CFD software. The aim of this part was to collect all necessary data that is required to build an aircraft's aerodynamic model that is going to be used for calculation of the trim conditions, dynamic stability and response to control. Therefore, both clean configurations and models with deflected control surfaces were computed. Moreover, cases with a quasi-pitch rotation were computed because they are needed to calculate the necessary stability derivatives. Detailed information about the numerical model, CFD software and computation set-up are presented in the section on the aerodynamics. The reference

**Figure 4** Top view presenting the wingspan definition and the front and rear flaps definition



Source: Figure by authors

values were the same for all the models and are presented in Table 1; the mass and moment of inertia were taken from Figat et al. (2010) and are result of the PPLANE project. The second step was calculation of the trim conditions. This part of the study was completed by the use of the optimisation process. The process based on the results obtained in the first step. The aircraft model was created under the assumption that each flap could be deflected separately, and the mutual impact on the aerodynamic characteristics is taken into account. The next step of this study was analysis of the stability that was conducted for all the configurations. Firstly, the static stability was analysed to select the flight conditions for the dynamic stability analysis. Then the dynamic stability of all configurations was computed to investigate whether a visible trend between the wingspan ratio and dynamic stability can be established. The last step was analysis of the aircraft response to control; separate deflections of the front and rear flaps were implemented. For the purpose of this research, a new parameter was established:  $b_F/b_R$  which is the ratio of the front wingspan to the rear wingspan. This parameter is used when results of different cases need to be compared. The list of all the considered cases is presented in Table 2.

### Aerodynamic computations

The aerodynamic characteristics were computed with use of the MGAERO (MGAERO, 2001) software. This software uses the Euler code with multigrid acceleration in the computation of the aerodynamic coefficients of an arbitrary configuration (Mavriplis, 1992). The numerical model was composed of a surface mesh and eight levels of multigrid blocks. The complete numerical model consisted of 8,200 on-body panels and 1,856,151 off-body panels. The deflection of flaps (front

**Table 1** Reference values and geometrical feature of the tandem wing aircraft

Parameter	Value	Unit
S	10.8	m <sup>2</sup>
MAC	2	m
Δs	1.5	[-]
m	1,600	kg
I <sub>y</sub>	6,400	kg m <sup>2</sup>

Source: Table by authors

**Table 2** List of computed cases

Case no.	$b_F/b_R$	$b_F$ [m]	$b_R$ [m]
1	0.64	4.20	6.60
2	0.69	4.40	6.40
3	0.74	4.60	6.20
4	0.80	4.80	6.00
5	0.86	5.00	5.80
6	0.93	5.20	5.60
7	1.00	5.40	5.40
8	1.08	5.60	5.20
9	1.16	5.80	5.00
10	1.25	6.00	4.80

Source: Table by authors

and the rear flaps) was modelled by rotation of the panel normal vector (MGAERO, 2001). All aerodynamic computations were made for the reference values presented in Table 1 and the following assumptions:

- The constant chord equals to  $c = 1.0$  m for both wings.
- The reference area is a sum of top view projections of the front wing's area and rear wing's area.
- The reference area is the same for all the considered cases.
- The position of the reference point was assumed to be located at the half distance between 25% of the chord of the front and rear wings (Figure 3). The change of the wingspan does not affect the position of the CG.
- The front and rear wingspan change are as shown in Table 2.

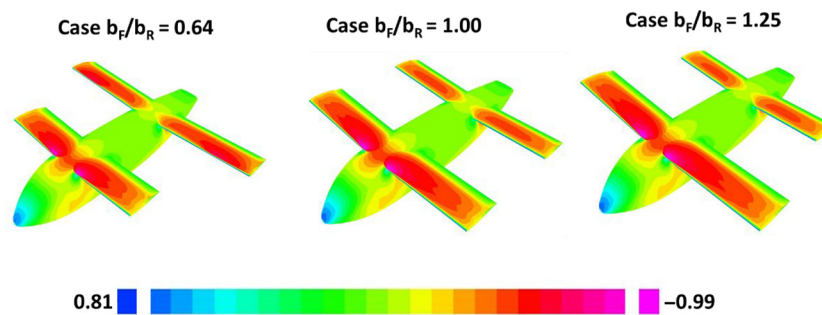
### Aerodynamic results

Firstly, the results of the clean configuration are presented. Figure 5 shows the  $C_p$  distribution computed by the MGAERO for three selected cases. The middle picture shows  $C_p$  for the case in where both wingspans are even, while the left and right pictures show the extreme cases when the ratio of the wingspans is the smallest ( $b_F/b_R = 0.640$ ) and the biggest ( $b_F/b_R = 1.25$ ).

Figure 6 shows the lift coefficient and pitching moment coefficient versus the angle of attack for three selected cases.

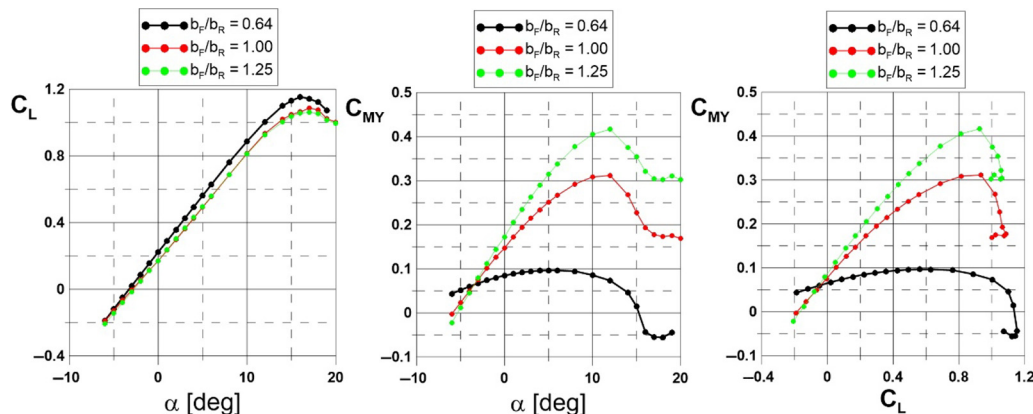
It can be observed that the aircraft configuration with the biggest rear wing has a significantly higher maximum lift coefficient than the remaining configurations. Moreover, the change in the maximum lift coefficient between the model with  $b_F/b_R = 0.640$  and  $b_F/b_R = 1$  is bigger than the difference between the model with  $b_F/b_R = 1.25$  and  $b_F/b_R = 1$ . Moreover, the configuration with the biggest rear wing is less statically unstable for low angles of attack. Figures 7 and 8 show the contribution of each wing to global aerodynamic characteristics; this is a key to understanding the significant difference in the pitching moment coefficient (Figure 6, plot on the right). The pitching moment is one of the key factors affecting the static and dynamic stability. In the case of  $b_F/b_R = 1$ , when both wingspans are even, the front wing generates more lift for positive AoA but achieves the critical AoA faster. The rear wing achieves the critical AoA later because the local AoA is affected by the front wing downwash and the rear wing is inclined at  $3^\circ$ . In the case of  $b_F/b_R = 0.64$ , the rear wing is more effective because its span is bigger than the front wing, resulting in the situation where only the selected part of the rear wing is affected by the front wing downwash. Moreover, the size of the rear wing is bigger, which is also associated with a bigger lift force. Figure 8 shows the pitching moment coefficient with respect to the angle of attack for the same three selected cases, while the rear wing generates stabilising pitching moment. The effectiveness of the rear wing is

Figure 5  $C_p$  distribution for three extreme configuration



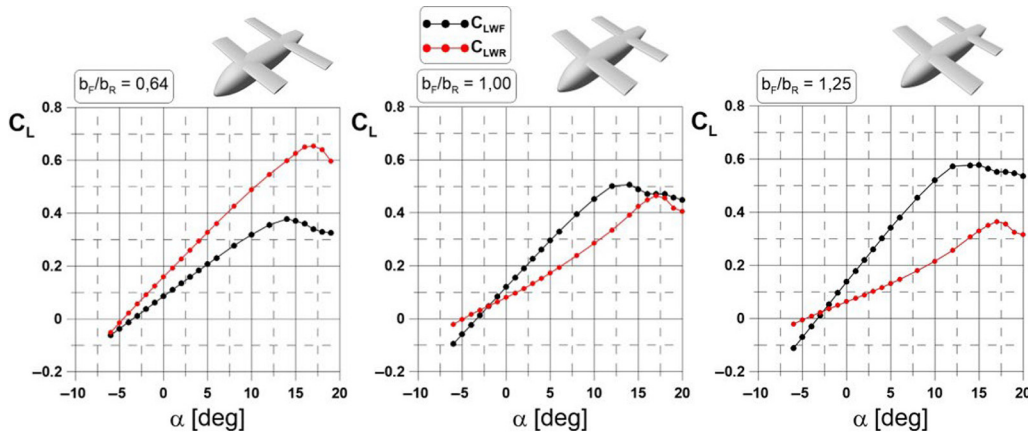
Source: Figure by authors

Figure 6 Lift (on the left) and pitching moment (in the middle) coefficients versus angle of attack for clean configuration pitching moment coefficient with respect to the lift coefficient for clean configuration (on the right)



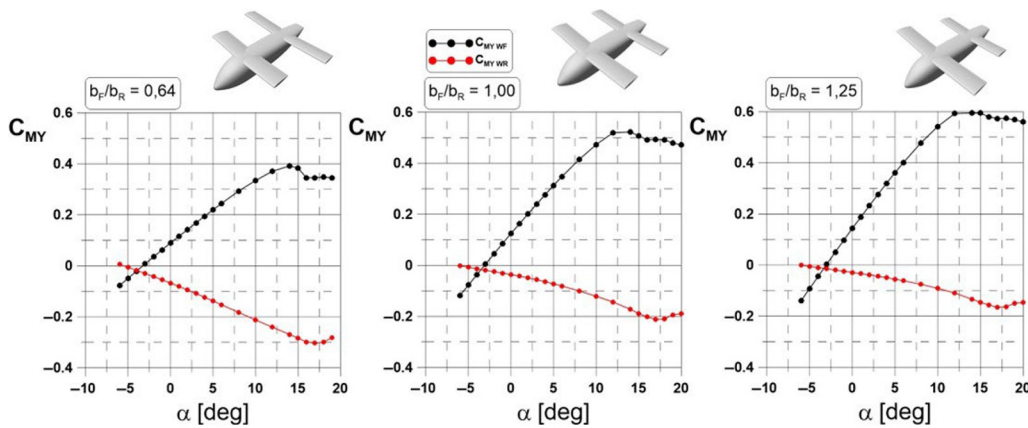
Source: Figure by authors

**Figure 7** Lift coefficient breakdown versus angle of attack for selected models. All coefficients are expressed with respect to the reference area (sum of both wing area)



Source: Figure by authors

**Figure 8** Pitching moment coefficient breakdown versus angle of attack for selected models. All coefficients are expressed with respect to the reference area (sum of both wing area)



Source: Figure by authors

associated with the lift: when the rear wing generates more lift, the pitching moment is bigger as well.

The aerodynamic impact of both (front and rear) flaps deflection was determined by control derivatives. The results obtained for all the considered cases are presented in Figure 9. It should be mentioned that the increment in the control derivatives mainly depends on the size of the flap which is changing with the change of the wingspan. In terms of lift generation, the front flap is more effective because the flow is less disturbed than in the case of the rear flap.

### Trim calculations

All the aerodynamic data obtained by CFD computations were used to build an analytical model of the aircraft longitudinal characteristics involving three basic equations (1)–(3):

$$\text{Lift coefficient } C_{L\text{TOTAL}} = f(\alpha, \delta_F, \delta_R) \quad (1)$$

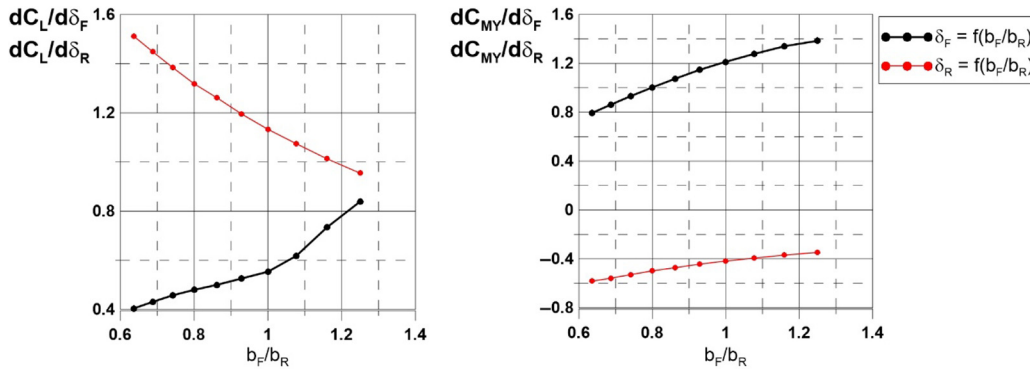
$$\text{Drag coefficient } C_{D\text{TOTAL}} = f(\alpha, \delta_F, \delta_R) \quad (2)$$

$$\text{Pitching Moment coefficient } C_{M\text{TOTAL}} = f(\alpha, \delta_F, \delta_R) \quad (3)$$

The main goal of the longitudinal control strategy is to find the flaps' deflections that give the best L/D ratio and satisfy the trim condition. To obtain the solution, the optimisation method was used. The optimisation algorithm was based on the steepest descent method which belongs to the deterministic gradient methods (Nocedal and Wright, 2006, Mieloszyk, 2017). To solve this problem, the objective function was defined by equation (4). It assumed the search of the trim condition with use of two independent flaps deflection. The optimisation problem is defined by equation (4). The results of different control strategies for aircraft with even wings are presented in Figat (2022):

$$\text{Minimise } F_{OBJ} = |C_M| + \frac{D}{L} \quad (4)$$

**Figure 9** Derivative of the lift force coefficient with respect to the flaps deflection (on the left) and derivative of the pitching moment coefficient with respect to flaps deflection (on the right). All derivatives are expressed in 1/rad



Source: Figure by authors

All the computations related to the trim condition were made with use of authoring script created in the MATLAB (MATLAB, 2022) software. Figure 10 shows the results of the flaps’ deflections versus AoA, satisfying the trim condition. The relations between the flaps’ deflections and angle of attack are nonlinear, which is associated with the strong aerodynamic coupling between wings. The reverse trend of the rear flap deflection for high angles of attack is caused by the front wing downwash. Figure 11 shows the lift to drag ratio obtained from the optimisation process; only results for selected models are plotted. Because of the mentioned strong aerodynamic coupling, it is impossible to create an analytical equation to predict the L/D based on the  $b_F/b_R$  and AoA.

### Derivatives computations

To solve the problem of the longitudinal dynamic stability, derivatives of lift force and pitching moment coefficient related to the pitch rate are required. Those dimensionless derivatives were computed based on the aerodynamic coefficients obtained with use of the MGAERO software and using the dimensionless angular rate defined by equation (5). It was assumed that all the dimensionless derivatives regarding the angular rate are computed for AoA = 0, and the impact of the AoA is neglected. Figure 12 shows the dimensionless derivative

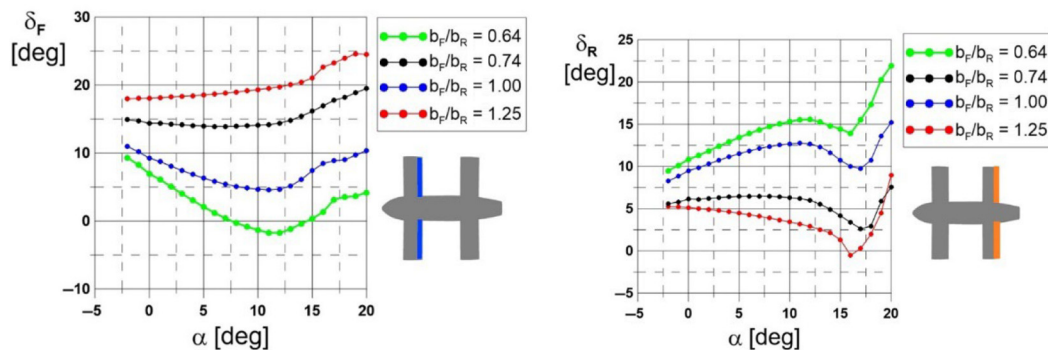
of the lift and pitching moment coefficient in respect to the pitch rate versus the span factor:

$$\hat{q} = \frac{q \cdot MAC}{2 \cdot V} \tag{5}$$

### Modelling of dynamic stability and control

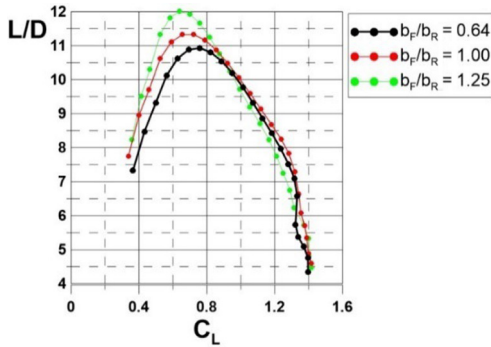
The dynamic stability and control computations were done with use of the MATLAB software, using an authoring script. The equations of aircraft motion were built in a state space form [equations (6) and (7)] (Cook, 1997; Nelson, 1998). Matrix A is the state matrix, while matrix B is the input matrix. The equations were linearised around the trim point using the small perturbation approach (Cook, 1997). The trim conditions were the outcome of the optimisation process, and as it was mentioned earlier, the results are nonlinear in respect to the span factor. Only longitudinal motion was considered so the equations were decoupled (Cook, 1997; Nelson, 1998). State vector x is expressed by equation (8) and includes four state variables axial (forward) speed U, normal (vertical) speed W, pitch rate q and pitch angle  $\theta$ . Figure 13 shows the definition of the linear and angular speeds. Moreover, the following assumptions were made:

**Figure 10** Front flap deflection  $\delta_F$  necessary to obtain trim conditions (on the left). Rear flap deflection  $\delta_R$  necessary to obtain trim conditions (on the right)



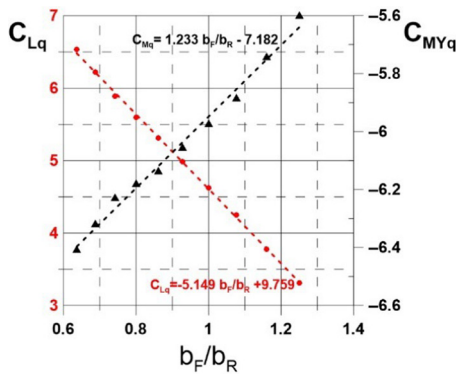
Source: Figure by authors

Figure 11 L/D ratio versus angle of attack under trim condition



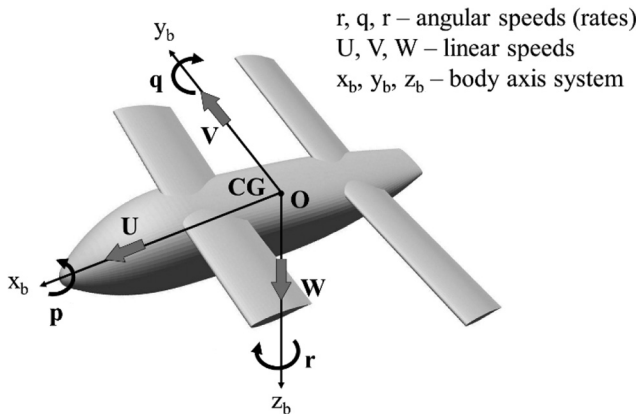
Source: Figure by authors

Figure 12  $C_{Lq}$  and  $C_{MYq}$  derivative versus span factor



Source: Figure by authors

Figure 13 Definition of the linear speeds, angular speeds and body axis system



Source: Figure by authors

- For all the considered models, the centre of gravity (reference point) is located at the same point – in the middle between 25% of the front and rear wing chord (Figure 3).

- The impact of the wingspan change on the position of the centre of gravity, mass and moment of inertia was neglected. All the calculations were computed for  $m = 1,600$  kg,  $I_Y = 6,400$  kg m<sup>2</sup> and fixed position of CG.
- The forces and moment were linearised around the trim point using stability and control derivatives. Only the first term was taken into account, while the higher order terms were neglected, including derivatives regarding the change of the normal velocity.
- Because of a low velocity, the impact of the Mach number was not considered ( $C_{LU}$ ,  $C_{DU}$ ,  $C_{MYU} = 0$ ).
- Calculations were done for  $H = 0$ , because the goal of this paper is to investigate the trend; therefore, flight altitude affects the value of dynamic parameters but not the trend itself:

$$\dot{x} = Ax + Bu \quad (6)$$

$$y = Cx + Du \quad (7)$$

$$x = [U, W, q, \theta]^T \quad (8)$$

$$u = [\delta] \quad (9)$$

Moreover, in the presented study, aerodynamic coefficients [equation (10)], the stability derivatives [equation (11)] and control derivatives [equations (12) and (13)] depended on the following parameters:

$$C_{L\alpha}, C_{D\alpha}, C_{MY\alpha} = f(\alpha, b_F/b_R) \quad (10)$$

$$C_{Lq}, C_{Dq}, C_{MYq} = f(b_F/b_R) \quad (11)$$

$$C_{L\delta F}, C_{D\delta F}, C_{MY\delta F} = f(b_F/b_R) \quad (12)$$

$$C_{L\delta R}, C_{D\delta R}, C_{MY\delta R} = f(b_F/b_R) \quad (13)$$

The input vector  $u$  only considers the response of flaps serving as an elevator in equation (9), so the single-input system was considered. In equation (7), matrix  $C$  is the output matrix, while matrix  $D$  is the direct matrix which is a zero matrix. The aircraft response to flaps deflection was analysed. Firstly, it was considered that the aircraft is in trim, then the step deflection of the front flap is commanded, while the rear flap does not change its deflection. Then the opposite case was considered.

### Static and dynamic stability results

Firstly, the result of the pitching moment coefficient versus the lift coefficient should be inspected to determine static stability. Such results are presented in Figure 6, and all the considered configurations are stable only for the high lift coefficient (around critical AoA). To ensure that all the models can be compared in the dynamic stability analysis, only a low speed (high AoA) was considered, and the selected speed is equal to 43.9 m/s. The next phase included comparison of the longitudinal dynamic stability of all the models. To determine

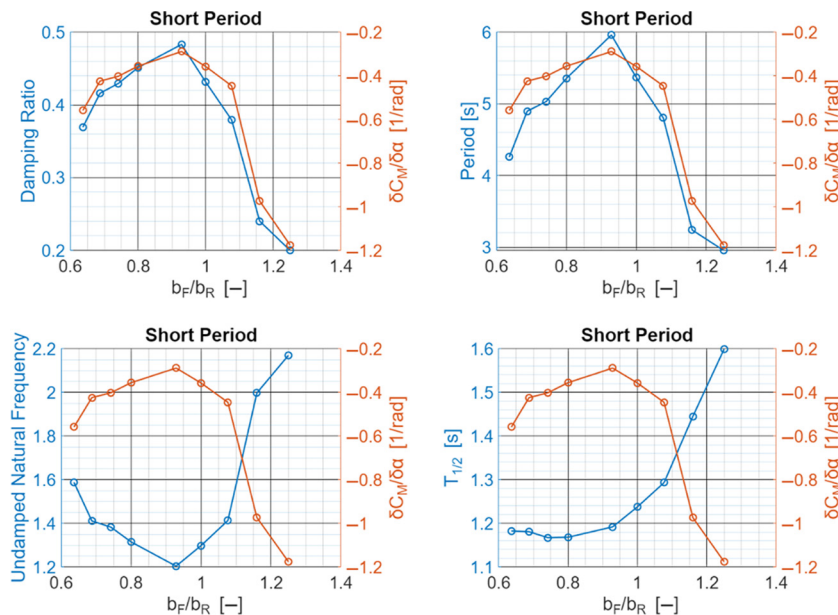


whether a visible trend between the dynamic stability and wingspan exists, the results were plotted against  $b_F/b_R$  parameter. Two modes of motion are analysed, the short period and the phugoid. In the case of the short period, the results are presented in Figure 14; the damping ratio, period, time to half damping and undamped natural frequency are nonlinear. The derivative of the pitching moment with respect to the angle of attack is also nonlinear, and its change matches the behaviour of the parameters that describe the aircraft dynamic stability. The nonlinear derivative of the pitching moment is caused by the strong aerodynamic coupling. The change of the pitching moment derivative is associated with the change of the wing size as well as with the mutual interference between wings caused by the downwash. Figure 15 presents the results for the phugoid motion that are also nonlinear. The airspeed is relatively low, and it can be assumed that the compressible effect is negligible; therefore, the change in the damping ratio should be associated with the change of  $L/D$ . Such a correlation of the nonlinear change of the  $L/D$  with respect to the span factor, and the phugoid parameters can be seen in Figure 15. This nonlinearity of the phugoid is directly associated with the trim condition. Because of a strong aerodynamic interference between the wings as well as different flaps efficiency caused by different sizes of the front and rear wing (with the span factor change), the obtained distribution of the  $L/D$  for the trim condition with respect to the span factor is nonlinear. This implies that, in the case of the design of the aircraft in the tandem wing configuration, the impact of the wingspan change on the trim cannot be predicted by a simple analytical expression. Especially the problem of the required deflection of the control surfaces to meet the trim condition must be numerically addressed each time when a new modification of aircraft geometry is implemented.

### Response to control

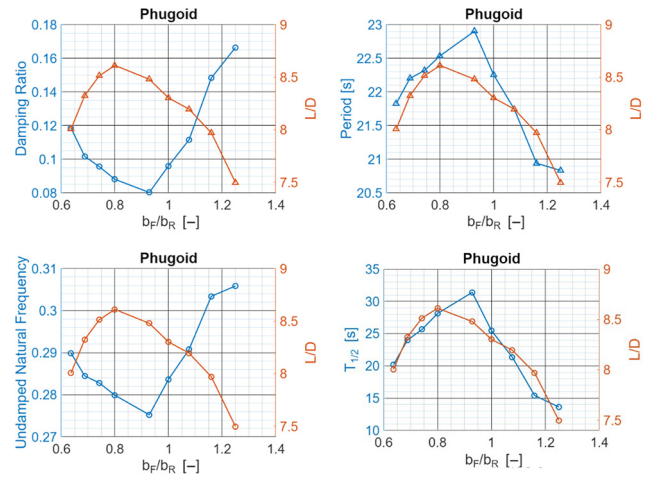
Two scenarios were considered; the first one was for the rear flap in the trim position and a step deflection of the front flap.

Figure 14 Short period results for all considered models, computation for airspeed equal to 43.9 m/s



Source: Figure by authors

Figure 15 Phugoid results for all considered models, computation for airspeed equal to 43.9 m/s

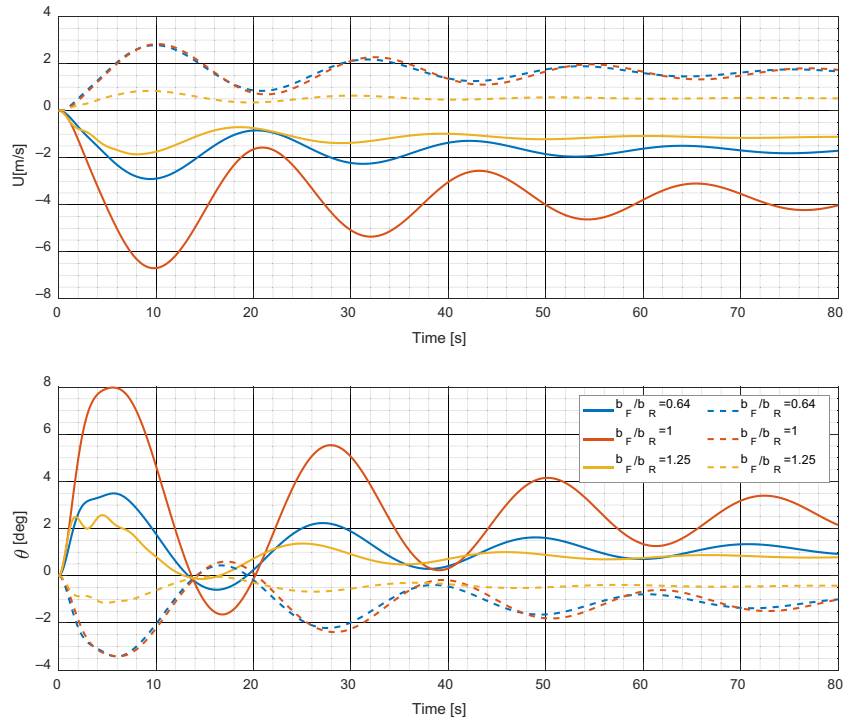


Source: Figure by authors

The second scenario was the opposite case; the front flap was in the trim position and the step deflection of the rear flap was engaged. All the presented results were computed by the MATLAB using the step function; two different flight conditions were considered. Figure 16 presents the results for computations with the initial flight condition which correspond to  $V = 43.9$  m/s and  $H = 0$  km. Figure 17 shows the results for computation with initial  $AoA = 13$  degrees and  $H = 0$  km. The plots present the change from the trim condition, with the solid line representing the front flap response, while the dotted line represents the rear flap response. The step deflection first induces the short period oscillations, then the phugoid motion occurs.

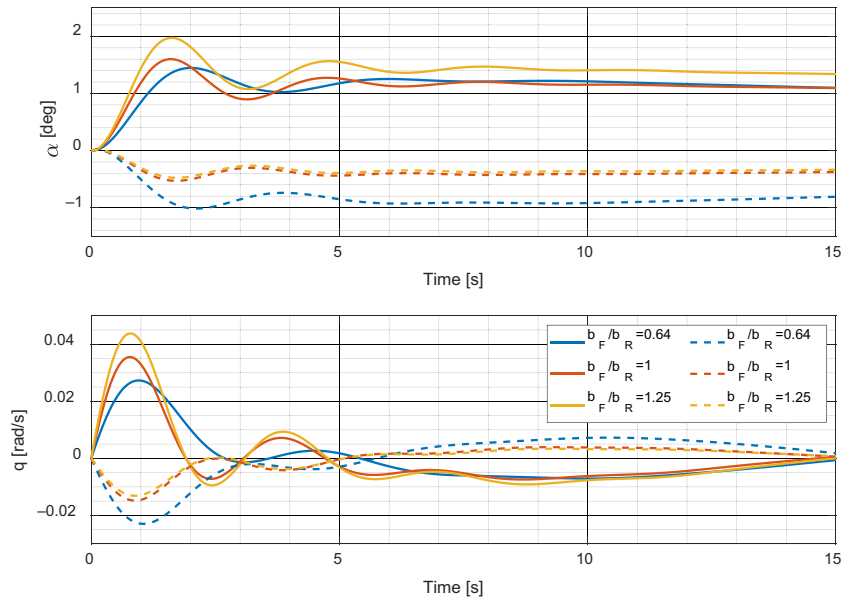
The results for the phugoid motion are analysed for the case when the initial speed is the same (Figure 16). In the case of

**Figure 16** Step response of the front flap (solid line) and rear flap (dotted line) for  $V = 43.9$  m/s



Source: Figure by authors

**Figure 17** Step response of the front flap (solid line) and rear flap (dotted line) for  $AoA = 13$  deg



Source: Figure by authors

the front flap response with respect to the rear flap response, the magnitude of the amplitude is bigger. The damping of the oscillation is associated with the lift to drag ratio which is nonlinear with respect to the span factor (Figure 15).

The results for the short period are analysed for the case when the initial angle of attack is the same. In the case of the front flap response with respect to the rear flap response, the magnitude of the amplitude is bigger. When the span factor decreases, the

oscillation damping increases, which is associated with the bigger size of the rear wing, which in turn is responsible for aircraft stabilisation. This can be observed in Figure 8 where the wings' contribution to the pitching moment is presented. If the results for the short period were analysed for the case of the fixed initial speed, then this effect would be difficult to identify because of a shift in the trim AoA.

## Conclusions

Computations of the aerodynamic, trim, dynamic stability and response to control were done for ten models of the tandem wing aircraft. Those models differed in respect to the span of both wings. Based on the obtained results, the following conclusions can be drawn:

- As it was expected, the results of the analysis showed the strong coupling effect in the considered set of configurations, especially noticeable for the trim condition.
- The flap deflection necessary for the trim condition significantly influenced the L/D ratio which is nonlinear with respect to the span factor.
- The span of wings (front and rear) significantly influenced the aircraft's pitching moment, because of the wings size (area) and aerodynamic coupling as well. Essentially, this influence is visible because of the aerodynamic impact (downwash) of the front wing on the rear wing.
- In the case of the tandem wing, because of a strong aerodynamic coupling, the optimisation cannot be limited to aerodynamics constrains.
- From the aerodynamic and stability point of view, the configuration with even wings is not the best choice.
- Because of a strong aerodynamic coupling, there is no clear trend between the span factor and static and dynamic stability properties. But just as for a classic aircraft, there is a strong relation between the short period and derivative of the pitching moment in respect to angle of attack; the phugoid properties and L/D. However, in the case of optimisation process, which would include dynamic stability constraint, it is necessary to compute dynamic stability properties for every model.
- The rear wing generates a stabilising pitching moment; therefore, the aircraft with a bigger rear wing is a better choice.
- The short period and phugoid oscillations generated by the step deflection of the front and rear flap were always damped.
- For the front flap, stronger magnitude of oscillation was observed.

## Further work

In the future, conducting analysis for more wing parameters including the inclination angle and gap is planned, as well as extending the analysis to lateral and directional modes of motion. Especially an optimisation process, engaging a more complex objective function that also takes into account stability constrains is intended.

## References

- Bottomley, A. (1977), "Comment", *Educational Administration*, Vol. 5 No. 2, pp. 27–28, doi: [10.1177/174114327700500205](https://doi.org/10.1177/174114327700500205).
- Bravo-Mosquera, P.D., Catalano, F.M. and Zingg, D.W. (2022), "Unconventional aircraft for civil aviation: a review of concepts and design methodologies", *Progress in Aerospace Sciences*, Vol. 131, p. 100813, doi: [10.1016/j.paerosci.2022.100813](https://doi.org/10.1016/j.paerosci.2022.100813).
- Brinkworth, B.J. (2016), "On the aerodynamics of the miles libellula tandem-wing aircraft concept", *Journal of Aeronautical History Paper*, Vol. 2, pp. 1941–1947.
- Cheng, H., Shi, Q., Wang, H., Shan, W. and Zeng, T. (2021), "Flight dynamics modeling and stability analysis of a tube-launched tandem wing aerial vehicle during the deploying process", *Proceedings of the Institution of Mechanical Engineers, Part G: Journal of Aerospace Engineering*, Vol. 236 No. 2, doi: [10.1177/09544100211010903](https://doi.org/10.1177/09544100211010903).
- Chou, H.Y., Liu, Y.C. and Hsiao, F.B. (2013), "The aerodynamic behavioral study of two wing's wake flow in tandem arrangement", *Procedia Engineering*, Vol. 67, pp. 1–14, doi: [10.1016/j.proeng.2013.12.001](https://doi.org/10.1016/j.proeng.2013.12.001).
- Cook, B.H. (1997), "Flight dynamics principles", Butterworth Heinemann, Canfield.
- Figat, M. (2022), "A strategy of the longitudinal control for the tandem wing configuration design", *Aircraft Engineering and Aerospace Technology*, doi: [10.1108/AEAT-12-2021-0372](https://doi.org/10.1108/AEAT-12-2021-0372).
- Figat, M., Goraj, Z. and Grendysa, W. (2010), "Preliminary concept for energetic model of pplane", In: presentation on PPLANE meeting, Madrid, 27–28 September 2010.
- Filho, A.C.D. and Belo, E.M. (2018), "Flight dynamics modeling and trim curves of a conceptual semi tandem wing vtol UAV", *Processing of 31st Congress of the International Council of the Aeronautical Sciences*, Brazil, Belo Horizonte, September 2019, pp. 9–14.
- Galinski, C., Krysztofiak, G., Miller, M., Ruchala, P., Kalski, M., Lis, M., Dziubinski, A., Bogdanski, K., Stefanek, L. and Hajduk, J. (2018), "Wind tunnel tests of the inverted joined wing and a comparison with CFD results", *Aircraft Engineering and Aerospace Technology*, Vol. 90 No. 4, pp. 586–601, doi: [10.1108/AEAT-11-2016-0195](https://doi.org/10.1108/AEAT-11-2016-0195).
- Gao, L., Li, C., Jin, H., Zhu, Y., Zhao, J. and Cai, H. (2017), "Aerodynamic characteristics of a novel catapult launched morphing tandem-wing unmanned aerial vehicle", *Advances in Mechanical Engineering*, Vol. 9 No. 2, doi: [10.1177/1687814017692290](https://doi.org/10.1177/1687814017692290).
- Goetzendorf-Grabowski, T. (2017), "Multi-disciplinary optimization in aeronautical engineering", *Proceedings of the Institution of Mechanical Engineers Part G: Journal of Aerospace Engineering*, Vol. 231 No. 12, pp. 2305–2313, doi: [10.1177/0954410017706994](https://doi.org/10.1177/0954410017706994).
- Goetzendorf-Grabowski, T. and Antoniewski, T. (2016), "Three surface aircraft (TSA) configuration – flying qualities evaluation", *Aircraft Engineering and Aerospace Technology*, Vol. 88 No. 2, pp. 277–284, doi: [10.1108/AEAT-02-2015-0055](https://doi.org/10.1108/AEAT-02-2015-0055).
- Goetzendorf-Grabowski, T. and Figat, M. (2017), "Aerodynamic and stability analysis of personal vehicle in tandem-wing configuration", *Proceedings of the Institution of Mechanical Engineers, Part G: Journal of Aerospace Engineering*, Vol 231, No. 11, doi: [10.1177/09544100166620](https://doi.org/10.1177/09544100166620).

- Goetzendorf-Grabowski, T. (2023), "Flight dynamics of unconventional configurations", *Progress in Aerospace Sciences*, Vol. 137, doi: [10.1016/j.paerosci.2023.100885](https://doi.org/10.1016/j.paerosci.2023.100885).
- Goraj, Z. (2014), "Flight dynamics models used in different national and international projects", *Aircraft Engineering and Aerospace Technology*, Vol. 86 No. 3, pp. 166-178, doi: [10.1108/AEAT-02-2013-0036](https://doi.org/10.1108/AEAT-02-2013-0036).
- Goraj, Z., Błaszczuk, P. and Goetzendorf-Grabowski, T. (1998), "Aerodynamika i dynamika konfiguracji dwupłata", *Transactions on Aerospace Research*, Vol. 98 No. 4, pp. 45-60.
- Goraj, Z., Frydrychewicz, A., Ransom, E.C.P., Self, A. and Wagstaff, P. (2001), "Aerodynamic, dynamic and conceptual design of a fire-fighting aircraft", *Proceedings of the Institution of Mechanical Engineers, Part G: Journal of Aerospace Engineering*, Vol. 215 No. 3, pp. 125-146. doi: [10.1243/0954410011533121](https://doi.org/10.1243/0954410011533121)
- Gudmundsson, S. (2014), *General Aviation Aircraft Design*, Butterworth-Heinemann, Oxford.
- Jinbin, F., Ji, S. and Huang, X. (2016), "The effects of design parameters on Tandem-Airfoil configuration aerodynamics", *The 2016 Asia-Pacific International Symposium on Aerospace Technology At: Toyama International Conference Center*, Toyama, Japan.
- Kostić, I., Tanović, D., Kostić, O., Abubaker, A.A.I. and Simonović, A. (2022), "Initial development of tandem wing UAV aerodynamic configuration", *Aircraft Engineering and Aerospace Technology*, doi: [10.1108/AEAT-06-2022-0149](https://doi.org/10.1108/AEAT-06-2022-0149).
- Masko, O.M., Kryvokhatko, I.S. and Sukhov, V.V. (2014), "Experimental research of tandem-scheme UAV model aerodynamic characteristics", *Transactions of the Institute of Aviation*, Vol. 237 No. 4, pp. 63-75.
- MATLAB (2022), available at: <https://ch.mathworks.com/products/matlab.html> (accessed 02 November 2022).
- Mavriplis, D.J. (1992), "Three-dimensional unstructured multigrid for the Euler equations", *Journal of Aircraft*, Vol. 30 No. 7.
- MGAERO (2001), "A cartesian multigrid Euler code for flow around arbitrary configurations – user's manual version 3.1.4".

- Mieloszyk, J. (2017), "Practical problems of numerical optimization in aerospace sciences", *Aircraft Engineering and Aerospace Technology*, Vol. 89 No. 4, pp. 570-578.
- Mieloszyk, J. and Goetzendorf-Grabowski, T. (2017), "Introduction of full flight dynamic stability constraints in aircraft multidisciplinary optimization", *Aerospace Science and Technology*, Vol. 68, pp. 252-260, doi: [10.1016/j.ast.2017.05.024](https://doi.org/10.1016/j.ast.2017.05.024).
- Mieloszyk, J., Tarnowski, A., Tomaszewski, A. and Goetzendorf-Grabowski, T. (2020), "Validation of flight dynamic stability optimization constraints with flight tests", *Aerospace Science and Technology*, Vol. 106, doi: [10.1016/j.ast.2020.106193](https://doi.org/10.1016/j.ast.2020.106193).
- Munk, M.M. (1922), "General biplane theory", NACA.
- Muyao, L. and Hongyi, X. (2021), "Investigation of aerodynamic interactions between NACA0012 airfoils in tandem", *Proceedings of 32nd Congress of the International Council of the Aeronautical Sciences*, China, Shanghai, pp. 6-10.
- Nelson, R.C. (1998), *Flight Stability and Automatic Control*, 2th ed., McGraw-Hill.
- Nocedal, J. and Wright, S. (2006), *Numerical Optimization*, Springer Science & Business Media, Berlin.
- Pobikrowska, K. and Goetzendorf-Grabowski, T. (2019), "Stability analysis of the experimental airplane powered by a pulsejet engine", *Aircraft Engineering and Aerospace Technology*, Vol. 91 No. 6, doi: [10.1108/AEAT-07-2018-0184](https://doi.org/10.1108/AEAT-07-2018-0184).
- PPLANE – the Personal Plane Project (2009), "Assessment and validation of pioneering concepts for personal air transport systems", Grant agreement no.: 233805, Annex 1, 30 June 2009.
- Stinton, D. (2001), *Design of the Aeroplane*, 2nd ed., Wiley-Blackwell, Hoboken.

### Corresponding author

Agnieszka Kwiek can be contacted at: [agnieszka.kwiek@pw.edu.pl](mailto:agnieszka.kwiek@pw.edu.pl)